High-responsivity, low-noise, room-temperature, self-mixing terahertz detector realized using floating antennas on a GaN-based field-effect transistor

J. D. Sun, Y. F. Sun, D. M. Wu, Y. Cai, H. Qin et al.

Citation: Appl. Phys. Lett. **100**, 013506 (2012); doi: 10.1063/1.3673617
View online: http://dx.doi.org/10.1063/1.3673617
View Table of Contents: http://apl.aip.org/resource/1/APPLAB/v100/i1
Published by the American Institute of Physics.

High-responsivity, low-noise, room-temperature, self-mixing terahertz detector realized using floating antennas on a GaN-based field-effect transistor

J. D. Sun (孙建东),[1,2,3] Y. F. Sun (孙云飞),[1,4] D. M. Wu (吴东岷),[1,4] Y. Cai (蔡勇),[1] H. Qin (秦华),[1,a)] and B. S. Zhang (张宝顺)[1,b)]
[1]*Key Laboratory of Nanodevices and Applications, Suzhou Institute of Nano-tech and Nano-bionics, Chinese Academy of Sciences, 398 Ruoshui Road, Suzhou, Jiangsu 215123, People's Republic of China*
[2]*Institute of Physics, Chinese Academy of Sciences, Beijing 100190, People's Republic of China*
[3]*Graduate University of Chinese Academy of Sciences, Beijing 100049, People's Republic of China*
[4]*i-Lab, Suzhou Institute of Nano-tech and Nano-bionics, Chinese Academy of Sciences, 398 Ruoshui Road, Suzhou, Jiangsu 215123, People's Republic of China*

(Received 27 July 2011; accepted 9 December 2011; published online 5 January 2012)

Using only optical lithography, we have fabricated a GaN/AlGaN high-electron mobility transistor with distinctive source and drain antennas electrically isolated from the electron channel. Working at room temperature, it efficiently detects terahertz radiation via self-mixing, with a responsivity (3.6 kV/W) exceptionally high for a III-V device and with a noise $(40\text{pW}/\sqrt{\text{Hz}})$ just above the thermal limit. Performance improves at 77 K. While the device itself is micrometer-sized, our modeling indicates the asymmetric antennas induce a rather localized (<200 nm) region of strong self-mixing. Thus, a nanometer-scale active region is achieved by design and without recourse to electron-beam lithography. © *2012 American Institute of Physics*. [doi:10.1063/1.3673617]

A frequency-converting solid-state mixer is one of the key devices in terahertz (THz) heterodyne transceivers. Schottky diodes and field-effect transistor (FET) based mixers are widely used in microwave and millimeter wave transceiver systems.[1,2] However, to extend the operating frequency into the THz range with high sensitivity, they encounter tremendous difficulties in reducing the electron transit time and various RC time constants mainly from the junction capacitance and the source/drain contact resistance. In FET-based devices, rich detection mechanisms/physics and (THz coupling) geometries can be utilized. Futhermore, THz sensing may occur in a very small fraction of the gated channel and so the parasitic circuit effects from source and drain contacts may be lessened (as will be shown in this report). From this point of view, FET-based THz mixers may offer better sensitivity than Schottky diodes.

In a high-electron mobility transistor (HEMT), plasmon excitation as a collective mode of the two-dimensional electron gas (2DEG) has been pursued for sensitive terahertz detection and spectroscopy since the 1980's.[3–5] As long ago as 1996, Dyakonov and Shur theoretically predicted and experimentally demonstrated that THz detection can be realized in a nano FET by resonant excitation of plasma waves when $\omega\tau \gg 1$ (here, ω is the THz frequency and τ is the plasmon relaxation time).[3] In the non-resonant regime $(\omega\tau \ll 1)$, damped plasma wave and mixing in the field-controlled resistive channel become the dominant effect.[6,7] Much attention has been paid to the design of the nanometer-sized field-effect channel, asymmetric source-gate-drain geometry,[8–14] and THz antennas (such as the patch antenna, dipole antenna, and log-periodic antenna).[9–11] In these detectors, the source/drain ohmic contacts are used as a plasmon-sensitive element and are directly connected to the antenna in the vicinity of the nano gate. However, the role of ohmic contacts is not yet fully understood, nor its optimization.[11,12] It would be interesting to try if it is possible to detect plasma wave without the need of local ohmic contacts. In a recent study by Dyer *et al.*,[10] multiple control gates were applied to manipulate individual plasmon cavities and the current-driven transport of plasma waves.

Here, we present high-responsivity THz self-mixing realized in a GaN/AlGaN HEMT detector using floating antennas and a 2 μm-long gate. It is worthwhile to state the similarities and differences between our previous related[7] and present detectors. Both utilize the same antenna design and self-mixing as the detection mechanism. Both are optimized for 900 GHz. The key difference lies in the implementation of the antennas and ohmic contacts. Previously, the source and drain antennas were connected directly to the channel. Now, the source and drain antennas are electrically isolated. Even though, the previous detector has a shorter gate length (0.7 μm), the new approach simultaneously offers better performance and simpler fabrication.

The device is fabricated on a GaN/AlGaN heterostructure, which provides a 2DEG about 33 nm below the surface. The electron mobility and the density at 300 K are $\mu = 1870$ cm^2/Vs and $n_s = 8.57 \times 10^{12}\,\text{cm}^{-2}$, respectively. Ultra-violet (UV), rather than electron-beam, lithography was used to define the detector pattern. A partial top view of the device is shown in Fig. 1(a). The gate length is $L = 2$ μm and the channel (mesa) width is $W = 8$ μm. Each antenna block is 45 $\mu\text{m} \times 10$ μm. Only the lower right antenna block (*g*-antenna) is connected (to the gate). The gap between the gate and the two isolated blocks (*i*-antennas) is 1.5 μm. The ohmic contacts are about 64 μm from the gate. The total thickness of the device including substrate is 416 μm. For characterization, a backward-wave oscillator (BWO: 780–950 GHz) was used in the same setup as described in Ref. 7.

a)Electronic mail: hqin2007@sinano.ac.cn.
b)Electronic mail: bszhang2006@sinano.ac.cn.

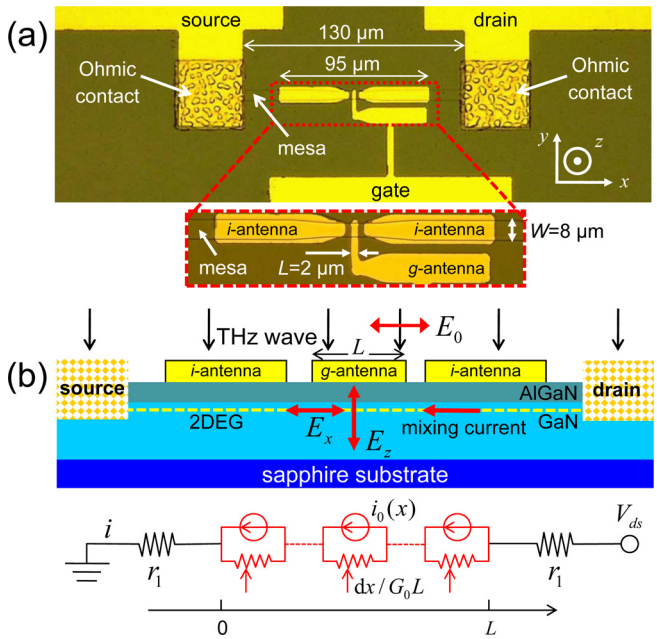

FIG. 1. (Color online) (a) Optical microscope images of the detector. Inset: The central gate region showing the isolated antenna (*i*-antenna) structures. (b) A schematic cross section and an equivalent circuit of the detector.

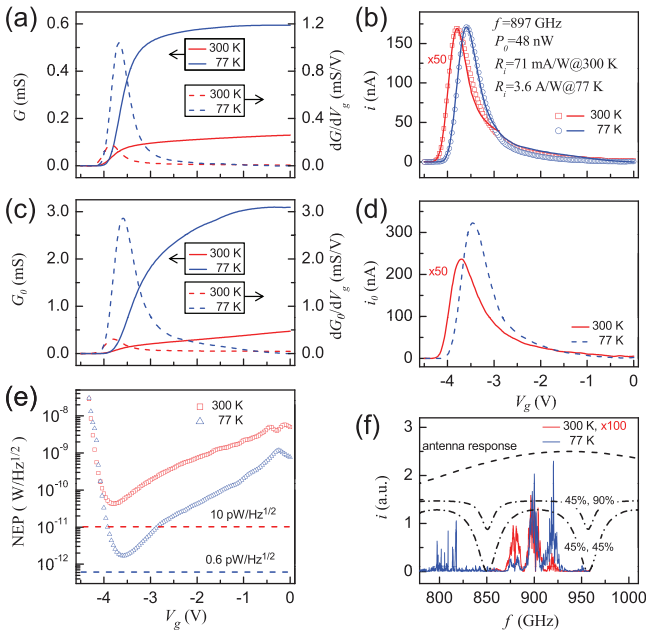

FIG. 2. (Color online) Self-mixing characteristics at 300 K and 77 K. From (a) to (e), different device parameters are given as a function of the gate voltage. (a) The measured source-drain conductance and its derivative. (b) The measured mixing current. (c) The deduced internal conductance and its derivative. (d) The deduced internal mixing current. (e) The measured NEP. The thermal-noise limited NEP at 300 K is marked by the upper dashed line and at 77 K by the lower dashed line. (f) The measured spectral response (full lines). The simulated antenna response (dashed line) and the substrate interference (dash-dotted lines). The refractive index of sapphire was taken to be 3.4. The reflectance at the top interface (air-GaN) is taken to be 45%, while that at the bottom interface is set to be 45% or 90%.

A schematic of the cross section of the device and an equivalent circuit are given in Fig. 1(b), where the resistances of the ohmic contacts and the long mesa are equally absorbed into $2r_1$. Upon THz irradiation of frequency $\omega = 2\pi f$ and energy flux P_0, both a horizontal $(E_x = \dot{\xi}_x E_0 \cos \omega t)$ and a perpendicular $(E_z = \dot{\xi}_z E_0 \cos(\omega t + \phi))$ electric field are induced in the electron channel beneath the gate by capacitive coupling, where E_0, $\dot{\xi}_x = d\xi_x/dx$, $\dot{\xi}_z = d\xi_z/dz$, and ϕ are the free-space THz electric field, the horizontal and perpendicular field enhancement factors, and the phase difference between the induced fields, respectively. E_0 is determined from the incident energy flux and the free-space impedance Z_0 by $P_0 = E_0^2/2Z_0$. The output short-circuit mixing current[15] can be written as

$$i = \frac{i_0}{1 + 2r_1 G_0} = \frac{1}{1 + 2r_1 G_0} \frac{dG_0}{dV_g} \int_0^L Z_0 P_0 \bar{z} \dot{\xi}_x \dot{\xi}_z \cos \phi dx, \quad (1)$$

where i_0 is the internal mixing current, $G_0 = \mu W C_g (V_g - V_{th})/L$ is the channel conductance, C_g is the gate-channel capacitance, V_g is the applied DC gate voltage, V_{th} is the threshold gate voltage, and $\bar{z} \approx \xi_z/\dot{\xi}_z$ is the effective distance between the gate and the 2DEG. The integral in Eq. (1) represents the overall antenna enhancement.

The source-drain conductance was characterized at 300 K and 77 K, as shown in Fig. 2(a). Upon THz irradiation of $f = 897$ GHz and estimated power[16] 48 nW, the mixing current as a function of the gate voltage is shown in Fig. 2(b). The corresponding maximum current responsivity (R_i) is estimated to be 71 mA/W and 3.6 A/W at 300 K and 77 K, respectively. The corresponding voltage responsivity (R_v) is 3.6 kV/W and 33.6 kV/W.[17] Shown as the solid lines in Fig. 2(b), the fitting curves based on Eq. (1) are in good agreement with the experimental data. The extracted internal conductance and internal mixing current are plotted in Figs. 2(c) and 2(d), respectively. The obtained circuit parameters are summarized in Table I. An enhancement factor of 51 in mixing current at 77 K relative to 300 K is observed, which is the combined effect of enhanced electron mobility, a decrease in series mesa resistance and an enhanced antenna efficiency: $0.80 \times 9.22 \times 7.2 \approx 51$. The increase in antenna efficiency ($\times 7.2$) is a result of the higher conductivity of gold and lower damping of GaN at 77 K.

The NEP of the detector as a function of the gate voltage was measured at 317 Hz with a bandwidth of 1.25 Hz. The results are shown in Fig. 2(e). The minimum NEP is as low as $40\text{pW}/\sqrt{\text{Hz}}$ and $2\text{pW}/\sqrt{\text{Hz}}$ at 300 K and 77 K, respectively. By way of comparison,[18] the thermal-noise limited NEP within the measurement bandwidth is about $10\text{pW}/\sqrt{\text{Hz}}$ at 300 K and $0.6\text{pW}/\sqrt{\text{Hz}}$ at 77 K. The room-temperature NEP is comparable to the best reports for zero-biased Schottky devices.[19] Our 77 K NEP is even comparable to the 4.2 K NEP of Si bolometers produced by IRLabs Inc.,[20] although our device is narrow-band and the bolometer is broadband. It has to be noted that a similar NEP has been achieved in field-effect transistors based on silicon CMOS technology,[21–24] although the optimum frequency was set around 650 GHz and 300 GHz.

The frequency response of the detector is shown in Fig. 2(f) over the BWO range. The observed frequency ranges 800–820 GHz and 870–920 GHz are narrower than the antenna response obtained from a finite-difference time-domain (FDTD) simulation. The interference of THz field at the device surface accounts for this discrepancy. A higher bandwidth would be achieved if the sapphire substrates were thinned to eliminate interference in the frequency range of concern.

TABLE I. Measured and fitting parameters at 300 K and 77 K.

Device[a]	T (K)	M (cm^2/Vs)	G_0 (mS)	$2r_1$ (kΩ)	$(1+2r_1G_0)^{-1}$ —	dG_0/dV_g (mS/V)	Integral[b] (10^{-6} V^2)	R_i (mA/W)	NEP (pW/$\sqrt{\text{Hz}}$)
OM	77	1.58×10^4	4.8×10^{-1}	1.4	0.60	2.86	109	3600	2
	300	1.87×10^3	5.9×10^{-2}	5.8	0.75	0.31	15	71	40
CM	300	1.87×10^3	1.2×10^{-1}	1.2	0.78	0.44	1	7.8	500
F_1	—	—	—	—	0.80	×9.22	×7.2	≈ 51	
F_2	—	—	—	—	0.96	×0.70	×15	≈ 9.1	

[a]OD and CD stand for the original detector and the control detector, respectively. Factor F_1 is the ratio of different quantities of the original detector at 77 K to that at 300 K. Factor F_2 is the ratio of different quantities of the original detector to the control detector at 300 K.
[b]The integral as shown in Eq. (1).

In Fig. 3(a), the simulated mixing factor is plotted to reveal the spatial distribution. For comparison, we simulated a control detector (CD) fabricated on the same substrate with the same dimensions for the antenna and the gate, but, unlike in the original detector, with the upper antenna blocks connected to the source/drain contacts. For both detectors, strong mixing occurs only at the edge of the gate. Due to the antenna asymmetry, the mixing at the left edge is about ×4 stronger than that at the right edge. Furthermore, the mixing at the left edge generates a positive current, opposite to that induced at the right edge. This inversion of polarity comes from a phase flip of 180°. This strongly unbalanced mixing creates the observed unidirectional mixing current. According to Eq. (1), a finite mixing current occurs only when the product of mixing fields and the derivative of the conductance are nonzero. We found more than half of the mixing current is generated within 200 nm of the right side of the gated channel, even though the gate is 10 times longer. The rest of the gated channel simply acts as a resistor in series with the mixing part. This means that the device is an inherently nanometer-sized detector at THz frequencies.

In Figs. 3(b) and 3(c), the measured conductance, its derivative, and the responsivity are compared to the control detector. The circuit parameters for the control detector are listed in Table I. Although the product of the scaling factor and the derivative of the conductance is about $0.96\times0.7\approx67\%$ of the control detector, the observed responsivity is enhanced by a factor of 9.1. This enhancement comes from the boost in antenna efficiency which is deduced to be ×15. However, as shown in Fig. 3(a), the FDTD simulation (without taking into account the realistic ohmic properties) suggests that the floating antennas provide an enhancement factor of only ×1.5. The enhancement mechanism is similar to that reported earlier using meander filters.[7] The strong discrepancy (a factor of 15/1.5 = 10) between the experimental data and the simulation indicates that the terahertz field is reduced by a factor of 10 due to the existence of local ohmic contacts (less conductive and rougher than pure gold antennas) in the control detector. This is not easily modeled in FDTD, due to the nature of the annealing process at high temperature, the uniformity and reproducibility of ohmic contacts are less controllable than floating gold antennas made by a standard lift-off process. The new design effectively avoids this difficulty and maintains the high efficiency of the original antenna.

In conclusion, we have set out a new approach to antenna implementation on self-mixing HEMT THz detectors, which at once simplifies fabrication and improves performance. The key is to electrically isolate the antennas from the electron channel. The current (and voltage) responsivity improves. The NEP is only ×4 above the thermal noise floor. The asymmetric geometry means that significant self-mixing is localized within a region of <200 nm, providing nanometer spatial

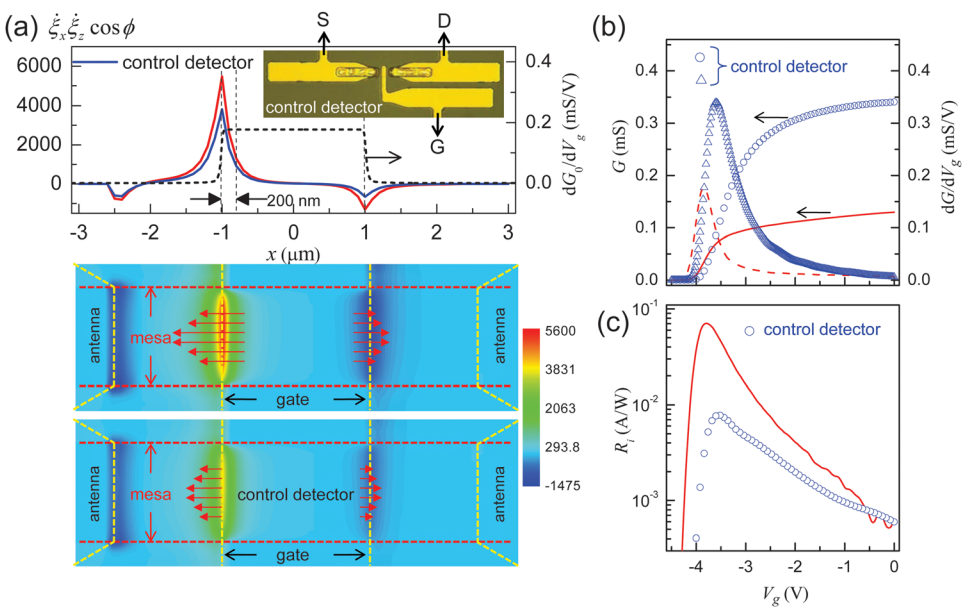

FIG. 3. (a) (Color online) The spatial distribution of the mixing factor from a FDTD simulation at 900 GHz compared to the control detector (shown in the inset of the top panel). A color-scale 2D plot for the detector (upper panel) and the control detector (lower panel). Comparison of the measured conductance, (b) its derivative and (c) the responsivity at 300 K.

sensitivity for a micrometer-sized device prepared simply by optical lithography.

This work was supported by the National Basic Research Program of China (973 Program) Grant No. G2009CB929303, the Knowledge Innovation Program of the Chinese Academy of Sciences Grant Nos. Y0BAQ31001 and KJCX2-EW-705, and the National Natural Science Foundation of China Grant No. 60871077, and Chinese Academy of Sciences visiting professorship for senior international scientists Grant No. 2010T2J07. The authors thank Professor Roger Lewis for insightful discussion and critically reading the manuscript.

[1]P. H. Siegel and R. J. Dengler, Int. J. Infrared Millim. Waves **27**, 465 (2006).
[2]E. Carey and S. Lidholm, "Monolithic mixer," in *Millimeter-Wave Integrated Circuits*, (Springer Science + Business Media, Inc. Boston, 2005), Chap. 6.
[3]M. I. Dyakonov and M. S. Shur, IEEE Trans. Electron Devices **43**, 380 (1996).
[4]X. G. Peralta, S. J. Allen, M. C. Wanke, N. E. Harff, J. A. Simmons, M. P. Lilly, J. L. Reno, P. J. Burke, and J. P. Eisenstein, Appl. Phys. Lett. **81**, 1627 (2002).
[5]I. V. Kukushkin, S. A. Mikhailov, J. H. Smeta, and K. von Klitzing, Appl. Phys. Lett. **86**, 044101 (2005).
[6]A. Lisauskas, U. Pfeiffer, E. Öjefors, P. H. Boliva, D. Glaab, and H. G. Roskos, J. Appl. Phys. **105**, 114511 (2009).
[7]Y. F. Sun, J. D. Sun, Y. Zhou, R. B. Tan, C. H. Zeng, W. Xue, H. Qin, B. S. Zhang, and D. M. Wu, Appl. Phys. Lett. **98**, 252103 (2011).
[8]W. Knap, Y. Deng, S. Rumyantsev, and M. S. Shur, Appl. Phys. Lett. **81**, 4637 (2002).
[9]T. Tanigawa, T. Onishi, S. Takigawa, and T. Otsuji, *Device Research Conference at South Bend,* IN, June 22, 2010, p. IV. A-9.
[10]G. C. Dyer, N. Q. Vinh, S. J. Allen, G. R. Aizin, J. Mikalopas, J. L. Reno, and E. A. Shaner, Appl. Phys. Lett. **97**, 193507 (2010).
[11]S. Kim, J. D. Zimmerman, P. Focardi, A. C. Gossard, D. H. Wu, and M. S. Sherwin, Appl. Phys. Lett. **92**, 253508 (2008).
[12]E. A. Shaner, M. Lee, M. C. Wanke, A. D. Grine, J. L. Reno, and S. J. Allen, Appl. Phys. Lett. **87**, 193507 (2005).
[13]D. Veksler, F. Teppe, A. P. Dmitriev, V. Yu. Kachorovskii, W. Knap, and M. S. Shur, Phys. Rev. B **73**, 125328 (2006).
[14]V. V. Popov, D. M. Ermolaev, K. V. Maremyanin, N. A. Maleev, V. E. Zemlyakov, V. I. Gavrilenko, and S. Yu. Shapoval, Appl. Phys. Lett. **98**, 153504 (2011).
[15]Inspired by a similar resistive mixing model and a more rigorous theory reported earlier in Refs. 3 and 6, respectively, we derived this equation from a quasi-static resistive FET mixer by taking into account the non-uniform THz field distribution. Even at sub-terahertz frequencies, this model agrees well with the experimental data. A detailed derivation and the experimental evidence for non-uniform THz field distribution will be presented in our extended paper elsewhere.
[16]The power sensed by the detector is estimated by raster scanning the beam pattern using both a commercial pyroelectric detector and the FET detector. The effective area of the detector is taken to be $200\,\mu\text{m} \times 200\,\mu\text{m}$, which is about 20 times greater than the total area of the antennas. Hence, the responsivity value obtained is a very conservative estimation.
[17]The voltage responsivity is measured experimentally. It can also be deduced from the current responsivity using $R_v = r \times R_i$, where r is the total resistance of the detector.
[18]The thermal limit was incorrectly stated in Ref. 7 to $1.08 \times 10^{-11}\text{nW}/\sqrt{\text{Hz}}$. The correct value is $1.08 \times 10^{-11}\text{W}/\sqrt{\text{Hz}}$.
[19]J. L. Hesler and T. W. Crowe, in *Proceeding of the 18th International Symposium on Space Terahertz Technology,* Edited by Alexandre Karpov (Pasadena, CA, March 2007), pp. 89–92.
[20]P. L. Richards, J. Appl. Phys. **76**, 1 (1994).
[21]H. Sherry, R. A. Hadi, J. Grzyb, E. Öjefors, A. Cathelin, A. Kaiser, and U. R. Pfeiffer, in *Radio Frequency Integrated Circuits Symposium* (IEEE, Baltimore, MD, 2011), pp. 365–368.
[22]S. Boppel, A. Lisauskas, V. Krozer, and H. G. Roskos, Electron. Lett. **47**, 661 (2011).
[23]E. Öjefors, N. Baktash, Y. Zhao, R. A. Hadi, H. Sherry, and U. R. Pfeiffer, in *Proceedings of the 36th European Solid-State Circuits Conference* (2010).
[24]F. Schuster, D. Coquillat, H. Videlier, M. Sakowicz, F. Teppe, L. Dussopt, B. Giffard, T. Skotnicki, and W. Knap, Opt. Express **19**, 7827 (2011).